Yubin Fu, Feng Qiu, Fan Zhang, Yiyong Mai, Yingchao Wang, Shibo Fu, Ruizhi Tang, Xiaodong Zhuang, Xinliang Feng

A dual-boron-cored luminogen capable of sensing and imaging

Erstveröffentlichung in / First published in:
Chemical Communications. 2015, 51(25), S. 5298--5301 [Zugriff am: 01.11.2019]. Royal Society of Chemistry. ISSN 1364-548X.

DOI: https://doi.org/10.1039/c4cc08551e

ChemComm

COMMUNICATION

View Article Online
View Journal | View Issue

Cite this: *Chem. Commun.*, 2015, 51, 5298

Received 29th October 2014,
Accepted 18th December 2014

DOI: 10.1039/c4cc08551e

www.rsc.org/chemcomm

A dual-boron-cored luminogen capable of sensing and imaging†

Yubin Fu,‡[a] Feng Qiu,‡[a] Fan Zhang,*[a] Yiyong Mai,[a] Yingchao Wang,[b] Shibo Fu,[b] Ruizhi Tang,[a] Xiaodong Zhuang[a] and Xinliang Feng*[ac]

A new dual-boron-cored luminogen ligated with a nitrogen-containing multidentate ligand and four bulky phenyl rings was readily synthesized. The unique molecular structure endows this BN-containing luminogen with rich photophysical properties in either solution or in the solid state, including a large Stokes shift, aggregation induced emission activity and reversible piezochromism. Furthermore, this BN-containing luminogen exhibits good capabilities for imaging living cells and sensing of fluoride anions.

BN-containing dyes, such as boron dipyrromethene (BODIPY), which exhibit high thermal stability, large charge carrier mobility and rich photophysical properties, have attracted increasing attention owing to their fundamental importance and potential applications in organic solar cells (OSCs), organic light-emitting diodes (OLEDs), sensing and imaging, *etc.*[1] However, these dye molecules mostly suffer from weakly emissive or nonemissive characteristics in concentrated solution or in the solid state because of their small Stokes shifts, favourable for the self-absorption from the heavy overlap between the absorption and emission spectra, or the aggregation-caused fluorescence quenching (ACQ) effect.[2]

Aggregation-induced emission (AIE) has been considered as an effective strategy to achieve high emission in concentrated solution or even in the solid state.[2b] Being structurally dependent on the molecular conformation or solid-state packing, an AIE luminogen may respond to a stimulation of mechanical performance, thus giving rise to the piezochromism behavior.[3] In contrast to the well-investigated AIE luminogens which are based on carbon-rich molecules, such as tetraphenylethene, AIE-active BN-containing luminogens remain rarely explored.

Boron-containing luminogens are widely used for sensing environmentally harmful fluoride ions, featuring low detection limits, high selectivity and low-cost. Typically, the luminescence response works through the following driving forces: (1) hydrogen bonding interactions; (2) anion–π interactions; (3) F^- direct binding to the boron atom; and (4) chemical reactions induced by F^-.[4] In this respect, searching for novel types of luminogens for fluoride anion sensing through a new responsive pathway has always been an attractive topic.[5]

Herein, we report a novel dual-boron-cored luminogen **5**, obtained by complexing 3,6-di(1*H*-pyrazol-1-yl)-1,2-diaminobenzene (**4**), a nitrogen-containing multidentate ligand, with triphenylborane. The geometric structure and photophysical properties of **5** were fully characterized. We further investigated the capabilities of **5** for imaging living cells and selective sensing of fluoride anions.

The target compound **5** was synthesized as shown in Scheme 1. The reaction of 2,1,3-benzothiadiazole (**1**) with bromine gave 4,7-dibromo-2,1,3-benzothiadiazole (**2**) in 88% yield. The key intermediate 4,7-di(1*H*-pyrazol-1-yl)benzo-[2,1,3]thiadiazole (**3**) was prepared in a yield of 72% by the copper iodide catalyzed reaction of **2** with pyrazole. Subsequently, compound **4** was obtained in quantitative yield upon reduction of **3** with $NaBH_4$. Finally, compound **4** and triphenylborane were treated in toluene under reflux conditions,

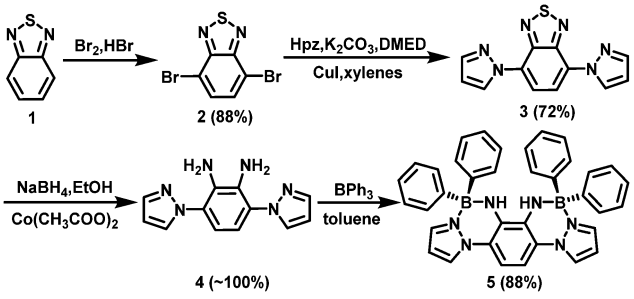

Scheme 1 Synthetic route towards compound **5**.

[a] *School of Chemistry and Chemical Engineering, State Key Laboratory of Metal Matrix Composites, Shanghai Jiao Tong University, Shanghai 200240, P. R. China. E-mail: fan-zhang@sjtu.edu.cn*

[b] *The first hospital Jilin University, College of Basic Sciences of Jilin University, Changchun 130021, P. R. China*

[c] *Department of Chemistry and Food Chemistry & Center for Advancing Electronics Dresden (cfaed), Technische, Universitaet Dresden, Mommsenstrasse 4, 01062 Dresden, Germany. E-mail: xinliang.feng@tu-dresden.de*

† Electronic supplementary information (ESI) available: Experimental details, optical spectra, DFT calculation, NMR spectra, and cellular imaging. CCDC 1031193. For ESI and crystallographic data in CIF or other electronic format see DOI: 10.1039/c4cc08551e

‡ These two authors contributed equally to this work.

affording the target BN-complex **5** in 88% yield. Compound **5** was fully characterized by ^{1}H, ^{13}C, ^{11}B NMR and HRMS spectroscopies (Fig. S1–S7, ESI†). In the ^{1}H NMR spectra, only one set of proton signals in the aromatic regions and one N–H peak at 3.97 ppm can be observed (Fig. S5, ESI†), suggesting a symmetric structure of **5**. Moreover, the ^{11}B NMR spectrum manifests a signal peak at −7.9 ppm (Fig. S7, ESI†), indicative of a four-coordinated state of the boron center.[6]

Single crystals of compound **5**, grown from acetone/*n*-hexane solution, were studied by single X-ray diffraction analysis (Fig. 1, Fig. S8 and S9, ESI†). The crystal structure reveals a five-ring fused conjugated aromatic framework, in which two boron atoms are deviated from the mean plane of the backbone. The dihedral angles defined by the middle benzene ring from two pyrazole rings are 7.9° and 24.5°, respectively. Such a twisted conformation can be attributed to the steric congestion caused by the bulky diphenyl groups decorated on each boron core. Two kinds of B–N bonds with the lengths of 1.51/1.52 Å and 1.61/1.62 Å coincide with their covalent and coordination bond nature, respectively.[7] In the packing diagram, the molecules organize in a staggered stacking pattern. The conjugated backbones of the neighbouring molecules are parallel to each other in an edge-to-edge fashion, with the shortest distances between the neighbouring molecules ranging from 3.35 to 3.95 nm. The intermolecular C–H$\cdots\pi$ interactions (2.814 Å) between the phenyl groups and conjugated backbones of the adjacent molecules can be identified (Fig. 1b).

The optical properties of compound **5** were investigated in CH_2Cl_2 at a concentration of 5×10^{-5} M (Fig. S10, ESI†). In the UV-vis spectra, three main absorption bands at 280, 329 and 394 nm were observed. The maximum absorption is typically attributed to the π–π^* transition of the aromatic skeleton.[8] When compound **5** was dissolved in higher polar solvents, the peak at 394 nm is gradually red shifted to 415 nm (Fig. S10, ESI†), indicating an intramolecular charge transfer (CT) transition. Thus, compound **5** can be polarized in the ground state. Such a phenomenon might be attributed to the multiple interactions between **5** and the solvent molecules, for instance, dipole–dipole, hydrogen bonding (through the N–H moiety) and π–π interactions.[9] This result agrees with the time-dependent density functional theory (TD-DFT) calculation, which reveals that the CT peak at 394 nm governs the electron transition from the highest occupied molecular orbital (HOMO) to the lowest unoccupied molecular orbital (LUMO) (Fig. S14, ESI†). The fluorescence spectrum of compound **5** shows a broad emission with a maximum peak at 486 nm, featuring a nonmirror image relative to the absorption spectrum. This suggests a lack of rigidity of the molecular scaffold.[10] Moreover, compound **5** in different solvents exhibits significant changes in emission maxima and intensity (Fig. S11, ESI†). The solvent-dependent emission of **5** probably arises from its acceptor–donor–acceptor (A–D–A) character. The dipole moment of the molecule will be affected by different polar solvents, leading to the different stability of the excited state. It should be emphasized that, the Stokes shift of 92 nm (2081 cm^{-1}) for **5** is among the largest values ever reported for BN-containing luminophores.[7] These results indicate a remarkable structural deformation between the ground and excited states of compound **5**, which would be beneficial to achieve high emission efficiency through effective weakening of self-absorption.

Encouraged by the unique photophysical properties of compound **5**, next we like to explore its stimuli-response behavior. The emission spectra of **5** in THF–water with different volumetric ratios of water were recorded, as shown in Fig. 2. In a THF solution, the fluorescence spectrum of **5** shows a flat line parallel to the abscissa, manifesting the poor fluorescence behavior. Interestingly, the fluorescence intensity increases rapidly when the water content is above 50% (v/v), and it reaches to a maximum value at 80% (v/v) fraction of water, but then decreases at higher fractions of water. These results strongly suggest a solvent-dependent AIE response.[2] To gain an insight into the aggregation behavior of compound **5**, the UV-vis spectra of **5** in THF–water solution with different volumetric ratios of water were recorded (Fig. S15, ESI†). The UV-vis spectra in aqueous THF with 80% and 90% of H_2O exhibit broadening absorption maxima with a levelling-off of long-wavelength tails, which are typically attributed to the formation of aggregates.[11,12] The aggregation behavior of **5** in THF–water was further supported by electron diffraction (ED) patterns and scanning electron microscopy (SEM) images. The ED patterns disclose an amorphous state for the sample formed in THF–water mixed solutions with 70% or 80% of H_2O. In contrast, a crystalline state was obtained in the case of the THF–water mixture with 90% of H_2O. This phenomenon is different from the crystallization-induced emission enhancement (CIEE) effect.[13]

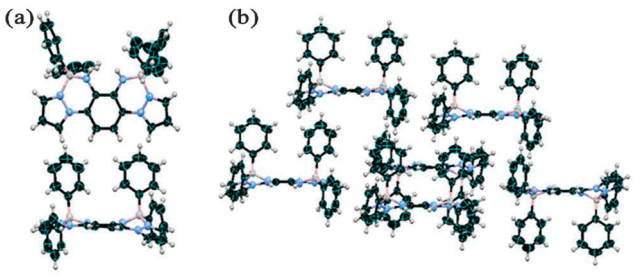

Fig. 1 (a) Thermal ellipsoid (50%) diagram of the molecular structure of **5**; (b) the crystal packing diagram of **5**. Solvent molecules are omitted for clarity.

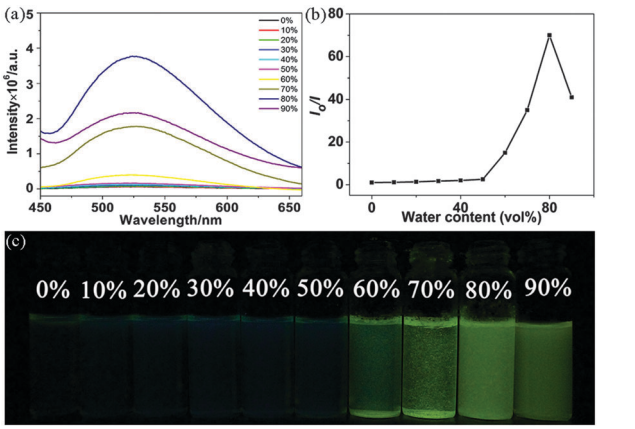

Fig. 2 (a) Fluorescence spectra of **5** in THF–water mixtures (1.0×10^{-3} M, excited at 413 nm) with varied volumetric fractions of water; (b) the fluorescence intensity change at different content of water; (c) the digital figures of **5** in THF–water mixtures under UV light (1.0×10^{-3} M, excited at 365 nm).

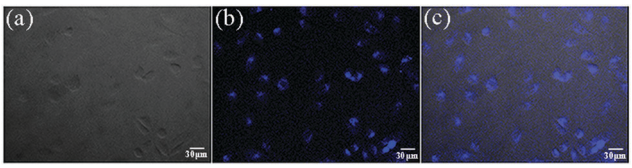

Fig. 3 Fluorescence microscopy images of HeLa cells incubated with compound **5** for 2 h: (a) a bright field image; (b) a fluorescence image; (c) a merged image.

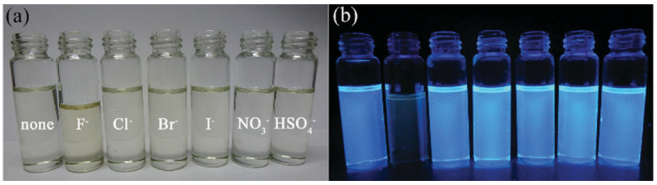

Fig. 5 Digital figures of compound **5** at a concentration of 5×10^{-5} M in DMSO under sunlight (a) and 365 nm UV light (b).

Compound **5** shows good photostability under the UV lamp (Fig. S18, ESI†). Moreover, the low *in vitro* cytotoxicity of **5** up to 100 μg mL^{-1} has been evaluated by MTT assay using NIH/3T3 normal cells (Fig. S19, ESI†). Thus, **5** with low cytotoxicity and AIE activity could be used as a potential tool for biological imaging. The cellular uptake of compound **5** was evaluated by fluorescence microscopy. As shown in Fig. 3, the strong blue fluorescence attributed to the aggregates of compound **5** was observed mainly in the cytoplasm of the cells with good distribution after culturing tumor cells with **5** for 2 h. With the increase of incubation time, the emission intensity in tumor cells increases (Fig. S20, ESI†), suggesting that the as-prepared nanoparticles were enclosed by the cell membranes, and then internalized by the cells. These results demonstrate that the structural feature of compound **5** with AIE activity is a good candidate for bioimaging applications.

Piezochromic luminogens generally refer to color changes under external pressure or mechanical grinding[3e,h] and have potential applications in optical recording devices, pressure sensors, damage detectors, *etc.*[3d,f] We consider that the sterically congested structure of compound **5** which plays a key role in its AIE activity, may render it responsive to mechanical stimuli. To this end, we ground the solid powder of **5** using a pestle. Interestingly, a change in emission color from green to yellow was observed under UV light at 365 nm (Fig. 4a and Fig. S21, ESI†). After one drop of dichloromethane was dropped onto the surface of the ground sample, the area where dichloromethane evaporated immediately recovered the original green color under UV light. Such reversible conversion of the emission colors of the as-prepared and ground samples can be successively repeated several times (>4), as shown in Fig. 4b. The red-shifted emission color after mechanical grinding indicates the change in intermolecular interaction in solid **5**. To confirm the optical results, the crystal packing of **5** was further investigated by X-ray diffraction (XRD) measurements. XRD patterns disclose that the as-prepared and ground samples of **5** feature crystalline and amorphous phases, respectively, which demonstrates the change in molecular packing during the grinding process.[3f] This result is also reversible by alternately grinding and soaking with CH_2Cl_2 (Fig. 4c).

The boron-cored structure of compound **5** also prompted us to examine its response to the stimuli of various anions. In the DMSO solution, compound **5** with a concentration of 5×10^{-5} M exhibits strong blue fluorescence which can be attributed to the high viscosity of the solvent. Further addition of F^- (5×10^{-3} M) resulted in an apparent color change from colorless to light yellow (Fig. 5). Moreover, UV-vis absorption revealed that a profile comprising two absorption maxima at 294 and 334 nm with remarkably enhanced intensity emerged when F^- was added, while the fluorescence was fully quenched (Fig. S22–S24, ESI†). In contrast, the addition of other anions (*e.g.* Cl^-, Br^-, I^-, NO_3^-, and HSO_4^-) did not cause obvious changes in the absorption and fluorescence spectra. To determine the sensitivity of **5** to F^- ions, the fluorescence titration experiment was carried out (Fig. S25, ESI†). With the incremental addition of F^-, the fluorescence intensity of **5** decreased progressively. The addition of 20 eq. of F^- resulted in complete fluorescence quenching. This pronounced fluorescence response of **5** to F^- ions at such a low concentration (Fig. S26, ESI†), is comparable to that of the best F^- detectors reported previously, such as triarylboranes and aryltrifluoroborate.[14]

In order to understand the mechanism of fluoride anion sensing, we further carried out ^1H NMR titration experiments of **5** in DMSO-d_6. Upon addition of F^-, pronounced shifts of the proton signals were observed (Fig. 6). Upon gradually increasing the amount of F^- from 1 to 6 eq., the well-resolved proton signals of the pyrazole ring (marked as H-a, H-b, H-d in Fig. 6a) and of the BN moiety (H-e) became weak and finally disappeared. Meanwhile, new proton signals at δ = 8.07, 7.77, 6.68 and 6.50 ppm emerged and their intensities increased. Strikingly, both chemical shifts and integration ratios of these new peaks are quite similar to the values of the protons in ligand **4** (Fig. 6). Thereby, it is reasonable to deduce that the new species with a similar chemical composition to ligand **4** were formed upon the addition of F^-. On the other hand, the proton signal of the BN moiety (H-e) at δ = 6.07 ppm in **5** disappeared after F^- titration, while a new high-field signal with the same integration intensity at δ = 5.28 ppm was observed, which is very close to that of

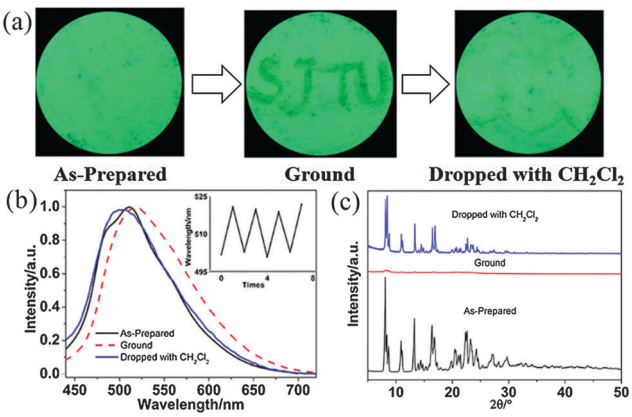

Fig. 4 (a) Photographic images of compound **5** after mechanical grinding under 365 nm UV light; (b) the solid fluorescence spectra of compound **5**, inset: repeated switching of the fluorescence emission maxima of the as-prepared and ground samples; (c) powder XRD patterns of compound **5**.

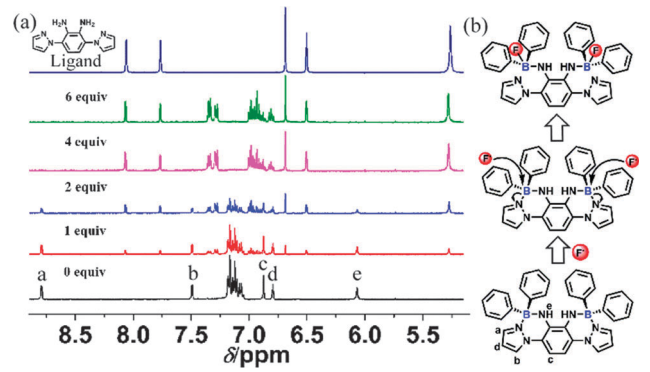

Fig. 6 (a) ^{1}H NMR spectra of boron compound **5** in DMSO-d_6 after the addition of various equivalents of TBAF; (b) schematic representation of a possible mechanism of the reaction between compound **5** and F^- in DMSO.

the proton in the imino group in **4** (δ = 5.26 ppm). These results suggest that the BN moiety is not fused in the aromatic backbone after the treatment with F^-. Moreover, the ^{11}B NMR spectrum of **5** treated with F^- shows a signal at δ = −5.73 ppm, which is characteristic of four-coordinated boron atoms (Fig. S27, ESI†).[6] On the basis of these analyses, we suggest a possible pathway of F^--stimuli response for **5**, as shown in Fig. 6b. Two F^- ions simultaneously attack the two Lewis acid boron centers of compound **5**, leading to the cleavage of the B–N coordination bond and the formation of the B–F bond. In other words, the two coordinated N atoms of pyrazole units in the ligand are released, while each boron core bearing two phenyl rings and one F atom is linked with the imino group through the B–N covalent bond. As a consequence, the original rigid conjugated backbone of compound **5** was destroyed, and the pyrazole unit with a released free lone pair of electrons on the N atom probably played a crucial role in quenching the fluorescence through the electron trapping effect.[15]

In summary, we have synthesized a novel BN-containing luminogen, featuring a sterically congested conformation and an extended π-conjugated system. Remarkably, this luminogen exhibits a large Stokes shift, AIE activity, reversible piezochromism behavior, *etc.* For a boron-based F^- detector, its boron center is required to be shielded with bulky substituents, *e.g.* the dury group.[16] In this work, the boron core is effectively protected by binding a pyrazole moiety through a weak B–N coordination bond, which can be readily cleaved upon treatment with F^-. Such a strategy holds great promise for designing new boron-based molecular dyes for sensing a wide range of ions.

We thank the Natural Science Foundation of China (NSFC 21174083, 2012CB933400, 2013CBA01600), the Shanghai Committee of Science and Technology (11JC1405400), the FNRS, China Postdoctoral Science Foundation (2013M540356). We thank Dr Manfred Wagner from Max Planck Institute for Polymer Research for NMR analysis, and Dr Wangzhang Yuan from Shanghai Jiao Tong University for kind discussion about the AIE effect and mechanochromism.

Notes and references

1 (*a*) M. J. G. Lesley, A. Woodward, N. J. Taylor, T. B. Marder, I. Cazenobe, I. Ledoux, J. Zyss, A. Thornton, D. W. Bruce and A. K. Kakkar, *Chem. Mater.*, 1998, **10**, 1355; (*b*) C. D. Entwistle and T. B. Marder, *Chem. Mater.*, 2004, **16**, 4574; (*c*) C. D. Entwistle and T. B. Marder, *Angew. Chem., Int. Ed.*, 2002, **41**, 2927; (*d*) S. Wang, *Coord. Chem. Rev.*, 2001, **215**, 79.

2 (*a*) X. Cheng, D. Li, Z. Zhang, H. Zhang and Y. Wang, *Org. Lett.*, 2014, **16**, 880; (*b*) Y. Hong, J. W. Y. Lam and B. Z. Tang, *Chem. Soc. Rev.*, 2011, **40**, 5361; (*c*) Y. Hong, J. W. Y. Lam and B. Z. Tang, *Chem. Commun.*, 2009, 4332.

3 (*a*) W. Liu, Y. Wang, M. Sun, D. Zhang, M. Zheng and W. Yang, *Chem. Commun.*, 2013, **49**, 6042; (*b*) D. Zhao, G. Li, D. Wu, X. Qin, P. Neuhaus, Y. Cheng, S. Yang, Z. Lu, X. Pu, C. Long and J. You, *Angew. Chem., Int. Ed.*, 2013, **52**, 13676; (*c*) Y. Sagara, T. Mutai, I. Yoshikawa and K. Araki, *J. Am. Chem. Soc.*, 2007, **129**, 1520; (*d*) Y. Sagara and T. Kato, *Nat. Chem.*, 2009, **1**, 605; (*e*) H. Bouas-Laurent and H. Dürr, *Pure Appl. Chem.*, 2001, **73**, 639; (*f*) K. Nagura, S. Saito, H. Yusa, H. Yamawaki, H. Fujihisa, H. Sato, Y. Shimoikeda and S. Yamaguchi, *J. Am. Chem. Soc.*, 2013, **135**, 10322; (*g*) X. Zhang, Z. Chi, J. Zhang, H. Li, B. Xu, X. Li, S. Liu, Y. Zhang and J. Xu, *J. Phys. Chem. B*, 2011, **115**, 7606; (*h*) Y. Dong, B. Xu, J. Zhang, X. Tan, L. Wang, J. Chen, H. Lv, S. Wen, B. Li, L. Ye, B. Zou and W. Tian, *Angew. Chem., Int. Ed.*, 2012, **51**, 10782; (*i*) X. Gu, J. Yao, G. Zhang, Y. Yan, C. Zhang, Q. Peng, Q. Liao, Y. Wu, Z. Xu, Y. Zhao, H. Fu and D. Zhang, *Adv. Funct. Mater.*, 2012, **22**, 4862; (*j*) N. Zhao, Z. Yang, J. W. Y. Lam, H. H. Y. Sung, N. Xie, S. Chen, H. Su, M. Gao, I. D. Williams, K. S. Wong and B. Z. Tang, *Chem. Commun.*, 2012, **48**, 8637; (*k*) Y. Dong, J. W. Y. Lam, A. Qin, Z. Li, J. Sun, H. H. Y. Sung, I. D. Williams and B. Z. Tang, *Chem. Commun.*, 2007, 40; (*l*) X. Luo, J. Li, C. Li, L. Heng, Y. Q. Dong, Z. Liu, Z. Bo and B. Z. Tang, *Adv. Mater.*, 2011, **23**, 3261.

4 (*a*) Y. Zhou, J. F. Zhang and J. Yoon, *Chem. Rev.*, 2014, **114**, 5511; (*b*) C. Saravanan, S. Easwaramoorthi, C.-Y. Hsiow, K. Wang, M. Hayashi and L. Wang, *Org. Lett.*, 2013, **16**, 354; (*c*) W.-M. Wan, F. Cheng and F. Jäkle, *Angew. Chem., Int. Ed.*, 2014, **53**, 8934.

5 (*a*) C. R. Wade, A. E. J. Broomsgrove, S. Aldridge and F. P. Gabbaï, *Chem. Rev.*, 2010, **110**, 3958; (*b*) A. Roy, D. Kand, T. Saha and P. Talukdar, *Chem. Commun.*, 2014, **50**, 5510.

6 (*a*) Y.-s. Guo, F. Zhang, J. Yang, F.-f. Wang, Y. NuLi and S.-i. Hirano, *Energy Environ. Sci.*, 2012, **5**, 9100; (*b*) S. Bieller, F. Zhang, M. Bolte, J. W. Bats, H.-W. Lerner and M. Wagner, *Organometallics*, 2004, **23**, 2107.

7 J. F. Araneda, W. E. Piers, B. Heyne, M. Parvez and R. McDonald, *Angew. Chem., Int. Ed.*, 2011, **50**, 12214.

8 (*a*) Y. Liu, F. Zhang, C. He, D. Wu, X. Zhuang, M. Xue, Y. Liu and X. Feng, *Chem. Commun.*, 2012, **48**, 4166; (*b*) Z.-H. Guo, T. Lei, Z.-X. Jin, J.-Y. Wang and J. Pei, *Org. Lett.*, 2013, **15**, 3530.

9 R. Li, S. Xiao, Y. Li, Q. Lin, R. Zhang, J. Zhao, C. Yang, K. Zou, D. Li and T. Yi, *Chem. Sci.*, 2014, **5**, 3922.

10 X. Wang, F. Zhang, J. Liu, R. Tang, Y. Fu, D. Wu, Q. Xu, X. Zhuang, G. He and X. Feng, *Org. Lett.*, 2013, **15**, 5714–5717.

11 (*a*) Y. Zhang, D. Li, Y. Li and J. Yu, *Chem. Sci.*, 2014, **5**, 2710; (*b*) X. Zhu, R. Liu, Y. Li, H. Huang, Q. Wang, D. Wang, X. Zhu, S. Liu and H. Zhu, *Chem. Commun.*, 2014, **50**, 12951.

12 C. He, D. Wu, F. Zhang, M. Xue, X. Zhuang, F. Qiu and X. Feng, *ChemPhysChem*, 2013, **14**, 2954.

13 (*a*) Y. Yang, X. Su, C. N. Carroll and I. Aprahamian, *Chem. Sci.*, 2012, **3**, 610; (*b*) Z. Zhao, S. Chen, X. Shen, F. Mahtab, Y. Yu, P. Lu, J. W. Y. Lam, H. S. Kwok and B. Z. Tang, *Chem. Commun.*, 2010, **46**, 686; (*c*) Y. Dong, *Aggregation-Induced Emission: Fundamentals and Applications*, John Wiley and Sons Ltd, 2013, vol. 1 and 2, p. 323; (*d*) L. Qian, B. Tong, J. Shen, J. Shi, J. Zhi, Y. Dong, F. Yang, Y. Dong, J. W. Y. Lam, Y. Liu and B. Z. Tang, *J. Phys. Chem. B*, 2009, **113**, 9098; (*e*) Y. Dong, J. W. Y. Lam, A. Qin, J. Sun, J. Liu, Z. Li, J. Sun, H. H. Y. Sung, I. D. Williams, H. S. Kwok and B. Z. Tang, *Chem. Commun.*, 2007, 3255; (*f*) Y. Jin, Y. Xu, Y. Liu, L. Wang, H. Jiang, X. Li and D. Cao, *Dyes Pigm.*, 2011, **90**, 311.

14 (*a*) J. O. Huh, H. Kim, K. M. Lee, Y. S. Lee, Y. Do and M. H. Lee, *Chem. Commun.*, 2010, **46**, 1138; (*b*) R. Ting, C. Harwig, U. auf dem Keller, S. McCormick, P. Austin, C. M. Overall, M. J. Adam, T. J. Ruth and D. M. Perrin, *J. Am. Chem. Soc.*, 2008, **130**, 12045; (*c*) M. Nicolas, B. Fabre and J. Simonet, *Electrochim. Acta*, 2001, **46**, 3421.

15 R. Tang, F. Zhang, Y. Fu, Q. Xu, X. Wang, X. Zhuang, D. Wu, A. Giannakopoulos, D. Beljonne and X. Feng, *Org. Lett.*, 2014, **16**, 4726.

16 W. Zhao, X. Zhuang, D. Wu, F. Zhang, D. Gehrig, F. Laquai and X. Feng, *J. Mater. Chem. A*, 2013, **1**, 13878.